Role of lamellar membrane structure in tether formation from bilayer vesicles

Bojan Božič,* Saša Svetina,* Boštjan Žekš,* and Richard E. Waugh‡
*Institute of Biophysics, Medical Faculty and "J. Stefan" Institute, University of Ljubljana, 61105 Ljubljana, Lipičeva 2, Slovenia; and ‡Department of Biophysics, University of Rochester School of Medicine and Dentistry, Rochester, New York 14642 USA

ABSTRACT A theoretical analysis is presented of the formation of membrane tethers from micropipette-aspirated phospholipid vesicles. In particular, it is taken into account that the phospholipid membrane is composed of two layers which are in contact but unconnected. The elastic energy of the bilayer is taken to be the sum of contributions from area expansivity, relative expansivity of the two monolayers, and bending. The vesicle is aspirated into a pipette and a constant point force is applied at the opposite side in the direction away from the pipette. The shape of the vesicle is approximated as a cylindrical projection into the pipette with a hemispherical cap, a spherical section, and a cylindrical tether with a hemispherical cap. The dimensions of the different regions of the vesicle are obtained by minimizing its elastic energy subject to the condition that the volume of the vesicle is fixed. The range of values for the parameters of the system is determined at which the existence of a tether is possible. Stability analysis is performed showing which of these configurations are stable. The importance of the relative expansion and compression of the constituent monolayers is established by recognizing that local bending energy by itself does not stabilize the vesicle geometry, and that in the limit as the relative expansivity modulus becomes infinitely large, a tether cannot be formed. Predictions are made for the functional relationships among experimentally observable quantities. In a companion report, the results of this analysis are applied to experimental measurements of tether formation, and used to calculate values for the membrane material coefficients.

INTRODUCTION

One of the primary functions of biological membranes is to provide a dynamic barrier for the compartmentalization of the cell and its contents. Thus, the mechanical behavior and deformability of membranes is of fundamental importance in understanding the dynamics of living cells. One of the more surprising shapes that membranes assume is that of an elongated cylinder with an aqueous core. Such structures are found in the Golgi apparatus and the endoplasmic reticulum. Their formation and dynamics have been documented using image-enhanced video microscopy of cells and cell extracts (Dabora and Sheetz, 1988; Cooper et al., 1990). Similar structures were first observed as the result of mechanical deformations of red blood cell membrane (Hochmuth et al., 1973). The mechanically-formed cylinders are called tethers, and have been formed and studied in both red blood cell membrane and phospholipid vesicles of different compositions (Hochmuth et al., 1982; Bo and Waugh, 1989; Waugh, 1982a, b; Song and Waugh, 1990). Although the elastic character exhibited by tethers was originally attributed to the membrane skeleton of the red blood cell (Evans and Hochmuth, 1976), it has been recognized subsequently that tether formation is characteristic of the membrane bilayer, and that the stability and elastic behavior of these structures is due to the elastic resistance of bilayer membranes to changes in their curvature (Waugh and Hochmuth, 1987). Thus, mechanically-formed tethers provide an unusual opportunity to study membrane curvature elasticity and to understand how membrane structure and composition can influence membrane behavior.

The elastic behavior of phospholipid membranes can be described as if they are two-dimensional liquids in the plane of the membrane and elastic bodies with respect to bending deformations (Evans and Needham, 1987). The effect of the lamellar structure of bilayer membranes on their bending properties has been considered by Evans (1974, 1980), who emphasized different bending behavior of systems with connected and unconnected constituent layers. In particular he showed, in the case of closed (or constrained at the edges) unconnected layers, where local adjustment and relative movement can take place between the layers, that the corresponding elastic energy depends on the integral of the curvature over the whole membrane. This was described as a nonlocal bending effect. The integral of the curvature over the whole membrane is proportional to the difference between the areas of the two layers. Thus, it is possible to relate the nonlocal bending energy to the "relative stretching" term introduced recently (Svetina

Address correspondence to Richard E. Waugh, Department of Biophysics, University of Rochester Medical Center, 601 Elmwood Avenue, Rochester, NY 14642.

et al., 1985). In this report we shall use the term "relative expansivity" to describe this contribution to the membrane energy.

In previous analyses of tether formation the contribution of the relative expansion of the two membrane layers has been neglected (Waugh and Hochmuth, 1987; Bo and Waugh, 1989). In this work we consider the importance of relative expansivity in tether formation and establish the analytical basis for obtaining the corresponding nonlocal bending modulus from the experimental data. The first section will provide the description of the mechanical properties of closed bilayers on which the analysis is based. Then an approximate geometric model for the aspirated tethered vesicle will be introduced, on the basis of which the elastic energy of the system can be determined approximately. The equilibrium tether configurations will be obtained by minimizing the free energy of the system, and criteria will be developed for the stability of the tether. The analytical framework will be used in a companion paper (Waugh et al., 1992) to calculate the nonlocal bending modulus from experimental observations.

Elastic properties of closed symmetric bilayer with unconnected layers

The two layers of a phospholipid bilayer are held in contact by hydrophobic forces but can be assumed to slide freely one by the other. Then the elastic properties of the bilayer are determined by the elastic properties of the individual constituent layers subject to the constraint that their areas are interrelated by:

$$A^{ex} = A^{in} + h \int (c_1 + c_2)\, dA_0. \tag{1}$$

Here A^{ex} and A^{in} are the areas of the external and the internal layers, respectively, at their neutral planes, h is the distance between these neutral planes, c_1 and c_2 are the two principal curvatures, and integration is over the area of the neutral plane of the bilayer, A_0. Following a more general treatment (Svetina et al., 1985), the elastic properties of the layers as separate entities ($m = 1, 2$) are described by their area expansivity modulus (K_m), their bending constant ($k_{c,m}$), and their spontaneous curvature $c_{0,m}$. The elastic energy of a closed symmetric bilayer composed of layers of the same composition (where therefore $K_2 = K_1$, $k_{c,2} = k_{c,1}$, and $c_{0,2} = -c_{0,1}$) is given by the sum of three terms:

(a) the area expansivity term takes the form:

$$\frac{1}{2} K(A - A_0)^2/A_0, \tag{2}$$

where K is the area expansivity modulus of the bilayer:

$$K = 2K_1, \tag{3}$$

and A is an expanded area of the neutral plane of the bilayer;

(b) the bending term is:

$$\frac{1}{2} k_c \int (c_1 + c_2)^2\, dA_0, \tag{4}$$

where k_c is the membrane bending modulus:

$$k_c = 2k_{c,1}, \tag{5}$$

and it has been recognized that in the case of symmetric bilayers the spontaneous curvature is zero;

(c) the relative expansivity term can be conveniently described by either of the two alternative expressions

$$\frac{1}{2}\frac{K_r}{A_0}(\Delta A - \Delta A_0)^2 = \frac{1}{2}\frac{k_r}{A_0}(\Delta A/h - \Delta A_0/h)^2. \tag{6}$$

It is clear from the first of these expressions that the relative expansivity term describes the energy of the membrane arising from the expansion and compression of the two membrane layers. It is manifested in that the difference between the areas of the inner and outer leaflets in the deformed state ($\Delta A = A^{ex} - A^{in}$) is different from the corresponding difference in the equilibrium state (ΔA_0). K_r is the relative expansivity modulus, which for a symmetrical membrane is equal to (Svetina et al., 1985)

$$K_r = K_1/2 = K/4. \tag{7}$$

The same membrane deformation can also be expressed (cf. Eq. 1) as the difference between the integral of the curvature over the membrane area in the deformed state ($\Delta A/h$) and in the equilibrium state ($\Delta A_0/h$). The corresponding energy term (the second expression in Eq. 6) involves as the elasticity modulus the nonlocal bending modulus k_r related to K_r by

$$k_r = h^2 K_r. \tag{8}$$

The moduli K_r and k_r are defined in such a way that they are intrinsic properties of the membrane. In this work the relative expansivity term will be expressed by the nonlocal bending modulus.

Analysis of tether formation

In the experimental procedure to be analyzed (Bo and Waugh, 1989), a vesicle is aspirated into a pipette, forming a spherical portion outside the pipette and a projection within the pipette. Then the vesicle is placed

into contact with a glass bead which sticks to it, i.e., a vesicle-bead pair is formed. After reducing the aspiration pressure the bead falls away from the vesicle, forming a tether between the bead and the body of the vesicle. The pressure can be adjusted to stop the bead movement, which means that equilibrium can be established. Reduction of the magnitude of the aspiration pressure causes the bead to move away from the vesicle drawing more material into the tether, whereas an increase in the magnitude of the aspiration pressure causes the bead to move toward the vesicle as material is drawn from the tether back onto the body of the vesicle. The length of the vesicle projection into the pipette changes accordingly.

The analysis involves the determination of the elastic energy of the membrane for a given configuration of the tethered vesicle (W_{el}), and the search for the configuration that corresponds to the minimum of the free energy of the system. The free energy (F) comprises the elastic energy (described above), the gravitational potential energy of the bead, and the contribution of the work done by the membrane due to hydrostatic pressure differences:

$$F = W_{el} - fx - \Delta p \pi R_p^2 L_p. \tag{9}$$

Here, f is the gravitational force of the bead, x is the distance from the pipette end to the bead, R_p the pipette radius, and L_p the vesicle projection into the pipette. $\Delta p = p_o - p_p$ is the difference between the external pressure outside the vesicle (p_o) and the pressure in the pipette (p_p), and is positive.

To determine W_{el}, the shape of the tethered vesicle is approximated by a simple geometrical model (Fig. 1). We consider only those contributions that change significantly in the course of varying the aspiration pressure and thus the configuration. To justify this approximation a more involved geometrical model is analyzed in Appendix 1. In that model, contributions to the elastic energy of all vesicle parts are taken into consideration. Comparison of the predictions of the two models shows that the simplifications used here are justified. The simplified shape of the tethered vesicle presented in Fig. 1 can be described by five parameters: pipette radius (R_p), the length of the vesicle projection into the pipette (L_p), radius of the spherical part of the vesicle (R_v), tether radius (R_t), and tether length (L_t). Four of these parameters are variable because R_p in a given experiment does not change. Due to the low permeability of phospholipid membranes to water, the vesicle volume (V_0) also does not change during the experiment. Thus the variables L_p and R_v are interrelated by the volume conservation equation valid for $L_p \geq R_p$:

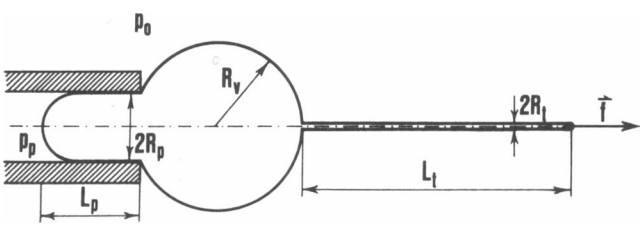

FIGURE 1 Schematic representation of the vesicle, which is aspirated in a pipette and pulled with constant force in the opposite direction. Notations given in the figure are: pipette radius (R_p), pipette projection length (L_p), vesicle radius (R_v), tether length (L_t), tether radius (R_t), the pressure surrounding the vesicle (p_0), the pressure in the pipette (p_p), and force pulling the tether (f).

$$V_0 = -\frac{\pi}{3}R_p^3 + \pi L_p R_p^2 + \frac{4\pi}{3}R_v^3. \tag{10}$$

In this expression we have neglected the volume of the tether because the tether radius is small ($R_t \ll R_p < R_v$).

The configuration of the tethered vesicle in the approximation used here thus involves only three free variables. These can be R_t, L_t, and R_v if L_p is by the use of Eq. 10 expressed in terms of R_v:

$$L_p = \frac{1}{\pi R_p^2}\left(V_0 + \frac{\pi}{3}R_p^3 - \frac{4\pi}{3}R_v^3\right). \tag{11}$$

The significant contributions to the elastic energy of the system shown in Fig. 1 are expected to be due to membrane area expansivity, relative expansivity due to changes of the tether length, and bending energy of the tether cylinder as demonstrated in Appendix 1. The changes in the area difference due to the contribution of other than tether parts of the vesicle are less than one percent of the contribution of the tether. This is valid even in the limit as the tether length becomes small, i.e., of the magnitude of only a few tether radii. Also, because changes in the value of R_v in the course of experiment are small, it is sufficient to consider only the length of the tether in the gravitational potential energy, and we can use L_t instead of x in the corresponding term. Then the functional to be minimized with respect to the three free variables reads

$$F = \frac{1}{2}\frac{K}{A_0}(A - A_0)^2 + \frac{2\pi^2 k_r}{A_0}(L_t - L_t^*)^2 + \pi k_c \frac{L_t}{R_t} - fL_t - \Delta p \pi R_p^2 L_p. \tag{12}$$

The area A is given by

$$A = -\pi R_p^2 + 2\pi L_p R_p + 4\pi R_v^2 + 2\pi L_t R_t. \tag{13}$$

In the relative expansivity term of Eq. 12 it is taken into consideration that the area difference of the constitutive vesicle (ΔA_0) is not necessarily the same as the area difference of the aspirated vesicle with the spherical external part (ΔA_i), i.e., the possibility exists that the areas of the layers of the aspirated vesicle may be relatively expanded (or compressed) before the tether is made. In view of this the deviation of the area difference from its equilibrium value ($\Delta A - \Delta A_0$) can be conveniently expressed as the difference between the value of such a deviation for the tether ($\Delta A - \Delta A_i$) and for the aspirated vesicle without the tether ($\Delta A_0 - \Delta A_i$). In Eq. 12 these two differences are defined in terms of the tether length $L_t = (\Delta A - \Delta A_i)/2\pi h$ and the parameter $L_t^* = (\Delta A_0 - \Delta A_i)/2\pi h$. The parameter L_t^* could have either a negative or positive value, depending on the vesicle history and the chemical environment inside and outside the vesicle.

To obtain the equilibrium tether configuration it is sufficient to determine the first derivatives of the free energy, Eq. 12, and set them to zero. These first derivatives are

$$\frac{\partial F}{\partial R_t} = \frac{K}{A_0}(A - A_0)A_t - \pi k_c \frac{L_t}{R_t^2} = 0, \tag{14}$$

$$\frac{\partial F}{\partial L_t} = \frac{K}{A_0}(A - A_0)A_L + \frac{4\pi^2 k_r}{A_0}(L_t - L_t^*) + \frac{\pi k_c}{R_t} - f = 0, \tag{15}$$

and

$$\frac{\partial F}{\partial R_v} = \frac{K}{A_0}(A - A_0)A_v + 4\pi R_v^2 \Delta p = 0, \tag{16}$$

where

$$A_t = \frac{\partial A}{\partial R_t} = 2\pi L_t \tag{17}$$

$$A_L = \frac{\partial A}{\partial L_t} = 2\pi R_t \tag{18}$$

and

$$A_v = \frac{\partial A}{\partial R_v} = -8\pi R_v\left(\frac{R_v}{R_p} - 1\right) \tag{19}$$

By suitably rearranging Eqs. 14 to 16 they read

$$\frac{K}{A_0}(A - A_0) - \frac{k_c}{2R_t^2} = 0, \tag{20}$$

$$\frac{2\pi k_c}{R_t} - f_{eff} + \frac{4\pi^2 k_r}{A_0} L_t = 0 \tag{21}$$

and

$$\Delta p - \frac{k_c}{R_t^2}\left(\frac{1}{R_p} - \frac{1}{R_v}\right) = 0. \tag{22}$$

Here we have incorporated the contribution due to constitutive area differences between the leaflets (L_t^*) into an effective force defined as

$$f_{eff} = f + \frac{4\pi^2 k_r}{A_0} L_t^*. \tag{23}$$

For practical purposes it is sufficient to analyze the tether formation under the assumption that the membrane area does not change, which is justified by the relatively large value of the area expansivity modulus (Appendix 1). Then we can determine the tether configuration by solving the set of equations 21, 22, and 13 in which we take $A = A_0$. It is first necessary to find the range of values for the system parameters over which tethers can form, and then to examine at which of these values the system is stable.

A possible representation of the system is obtained by introducing as a new variable the product $L_t R_t$. By eliminating L_p from the Eqs. 10 and 13, this product can be expressed in terms of the vesicle radius R_v:

$$L_t R_t = \frac{R_p^2}{6} + 2R_v^2\left(\frac{2R_v}{3R_p} - 1\right) - \frac{1}{\pi}\left(\frac{V_0}{R_p} - \frac{A_0}{2}\right). \tag{24}$$

Then by eliminating the tether radius R_t from Eqs. 21 and 22 and using Eq. 24, a single equation is obtained from which the vesicle radius can be determined

$$\frac{4\pi^2 k_c \Delta p}{f_{eff}^2} = \frac{\frac{1}{R_p} - \frac{1}{R_v}}{\left\{1 + \frac{2\pi k_r}{A_0 k_c}\left[\frac{R_p^2}{6} + 2R_v^2\left(\frac{2R_v}{3R_p} - 1\right) - \frac{1}{\pi}\left(\frac{V_0}{R_p} - \frac{A_0}{2}\right)\right]\right\}^2}. \tag{25}$$

Tether configurations are possible where a solution of Eq. 25 exists. It is of interest to determine at what values of the model parameters Eq. 25 has a solution. This can be done conveniently for a vesicle with an arbitrary membrane area if all the lengths appearing in Eq. 25 are measured relative to the radius of the sphere with area A_0: $R_0 = (A_0/4\pi)^{1/2}$. The parameters entering this equation are then the relative volume ($v = 3V_0/4\pi R_0^3$), the relative pipette radius (R_p/R_0), the ratio between the nonlocal bending modulus and the bending modulus ($q = k_r/k_c$), and the dimensionless pressure difference defined as

$$\Delta P = \frac{4\pi^2 k_c \Delta p R_0}{f_{eff}^2}. \tag{26}$$

In Fig. 2 is shown for given values of v and R_p/R_0 the region in the $\Delta P/q$ diagram in which tether configurations are possible. This region is essentially bounded by

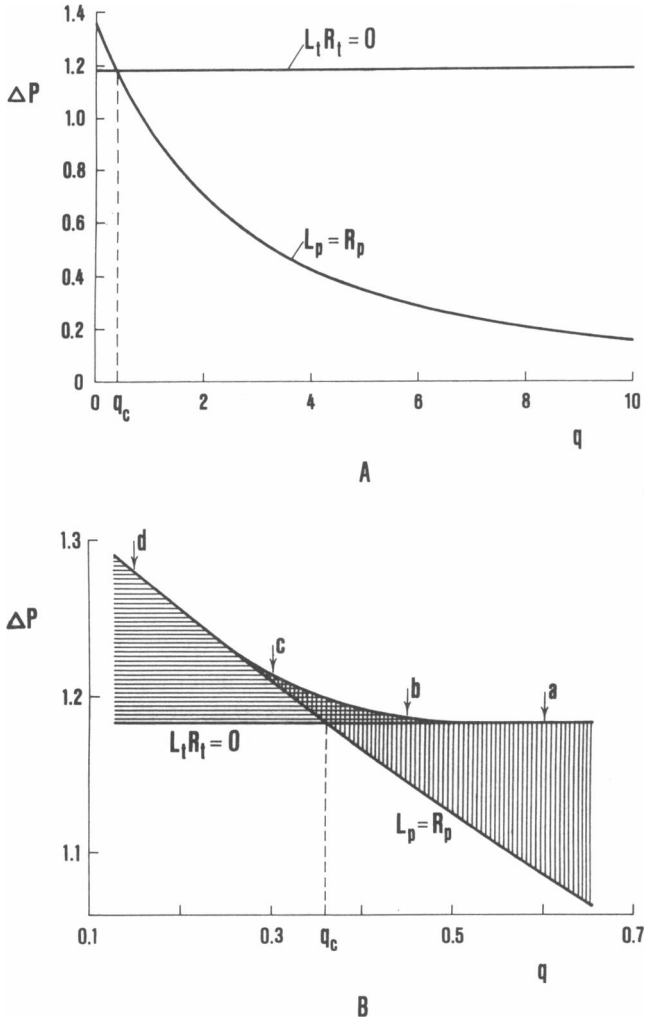

FIGURE 2 The diagram shows the values of the dimensionless parameter ΔP and ratio $q = k_r/k_c$ at which tether configurations are possible for a vesicle with the relative volume $v = 0.7$ and relative radius of the pipette $R_p/R_0 = 0.4$. (*A*) The dependence of the dimensionless parameter ΔP on q for $L_tR_t = 0$ obtained by eliminating R_v from Eqs. 24 and 27, and for $L_p = R_p$ obtained by eliminating R_v from Eqs. 11 and 25. Tether configurations exist essentially between these two curves except in close vicinity of q_c, which denotes crossing of these two curves. (*B*) The detailed presentation of the region close to q_c, where there is the transition between the stable and unstable tether configurations. The horizontally shaded area shows at which values of ΔP and q there are unstable configurations, and the vertically shaded area shows where there are stable configurations. Within the cross-hatched area there are two solutions one corresponding to the stable and one to the unstable configurations. The arrows denote values of q at which the product L_tR_t as a function of ΔP is presented in Fig. 3.

two lines: the line where pipette length is equal to pipette radius and the line where the tether length is zero, i.e., where the product L_tR_t is zero. (We assume that the cylindrical approximation for the tether is good if L_t is larger than $\sim 10\ R_t$. We estimated that the ΔP values obtained for such minimal tethers ($L_t = 10\ R_t$) differ from the values obtained for $L_tR_t = 0$ by less than 10^{-4} of their values.) The former line is obtained from Eq. 25 by inserting the value for R_v obtained from Eq. 11 with $L_p = R_p$. The latter line is a constant, because in the case $L_tR_t = 0$, Eq. 25 reduces to

$$\frac{4\pi^2 k_c \Delta p}{f_{\text{eff}}^2} = \frac{1}{R_p} - \frac{1}{R_v}. \tag{27}$$

(R_v does not depend on q as can be seen from Eq. 24.) Tether configurations exist in the region between these two lines (Fig. 2 *A*), however, there is another small region in the close vicinity of the point where they intersect ($q = q_c$). Within this region (it is shown in Fig. 2 *B* by the cross-hatched area) Eq. 25 has actually two solutions. That means that for an arbitrary pair of parameters q and ΔP from the cross-hatched area two values for the radius R_v can be obtained corresponding to two different tether configurations. (A third root of Eq. 25 also exists but in the nonphysical regime, $L_t < 0$.)

It is appropriate at this point to consider the stability of these equilibrium solutions. We analyze the stability of the system by determining the second derivatives of the free energy, Eq. 12. The matrix of second derivatives $\partial^2 F/\partial x_i \partial x_j$, where x_i and x_j denote consecutively R_t, L_t, and R_v, is

$$\mathbf{M} = \begin{vmatrix} \frac{2\pi k_c L_t}{R_t^3} + \frac{K}{A_0}A_t^2 & \frac{K}{A_0}A_tA_L & \frac{K}{A_0}A_tA_v \\ \frac{K}{A_0}A_tA_L & \frac{4\pi^2 k_r}{A_0} + \frac{K}{A_0}A_L^2 & \frac{K}{A_0}A_LA_v \\ \frac{K}{A_0}A_tA_v & \frac{K}{A_0}A_LA_v & -\frac{4\pi k_c}{R^2} + \frac{K}{A_0}A_v^2 \end{vmatrix}. \tag{28}$$

The system is stable provided that the eigenvalues of this matrix are all positive. The eigenvalues are roots of the equation

$$\det|\mathbf{M} - \lambda\mathbf{I}| = 0 \tag{29}$$

where $\mathbf{I}$ is the unit matrix. The resulting cubic equation can be conveniently expressed as

$$-\lambda^3 + \lambda^2\left(p_1 + \frac{K}{A_0}p_2\right) - \lambda\left(p_3 + \frac{K}{A_0}p_4\right) + p_5 + \frac{K}{A_0}p_6 = 0, \tag{30}$$

where

$$p_1 = \frac{2\pi k_c L_t}{R_t^3} + \frac{4\pi^2 k_r}{A_0} - \frac{4\pi k_c}{R_t^2} \tag{31}$$

$$p_2 = A_t^2 + A_L^2 + A_v^2 \tag{32}$$

$$p_3 = \frac{8\pi^3 k_c k_r}{R_t^2 A_0}\left(\frac{L_t}{R_t} - 2\right) - \frac{8\pi^2 k_c^2 L_t}{R_t^5} \tag{33}$$

$$p_4 = A_t^2\left(\frac{4\pi^2 k_r}{A_0} - \frac{4\pi k_c}{R_t^2}\right) + A_L^2\left(\frac{2\pi k_c L_t}{R_t^3} - \frac{4\pi k_c}{R_t^2}\right) + A_v^2\left(\frac{4\pi^2 k_r}{A_0} + \frac{2\pi k_c L_t}{R_t^3}\right) \tag{34}$$

$$p_5 = -\frac{32\pi^4 k_c^2 k_r L_t}{R_t^5 A_0} \tag{35}$$

$$p_6 = -\frac{16\pi^3 k_t k_c}{A_0 R_t^2} A_t^2 - \frac{8\pi^2 k_c^2 L_t}{R_t^5} A_L^2 + \frac{8\pi^3 k_t k_c L_t}{A_0 R_t^3} A_v^2 \tag{36}$$

One of the roots of Eq. 30 is proportional to the area expansivity modulus K. For large values of K this root becomes equal to Kp_2/A_0 and is therefore positive because p_2 (Eq. 32) is positive. It is of interest to inspect the sign of the other two roots. We take advantage of the fact that the expansivity modulus K is large in comparison to other constants appearing in Eq. 30. By dividing Eq. 30 by K and neglecting the terms in it proportional to $1/K$ we get a quadratic equation:

$$p_2\lambda^2 - p_4\lambda + p_6 = 0, \tag{37}$$

the roots of which correspond to the two roots of Eq. 30 that are not proportional to K. The roots of Eq. 37 are positive if the third term (p_6) in Eq. 37 is larger than zero (because it can be shown that the parameter p_4 is always positive if p_6 is positive). The criterion for the stability of the tether configuration can then be conveniently expressed by inserting into Eq. 36 the expressions 17 to 19 as

$$8k_r R_v^2\left(\frac{R_v}{R_p} - 1\right)^2 - k_r R_t L_t - \frac{k_c A_0}{2\pi} > 0. \tag{38}$$

We apply this stability criterion to the solutions illustrated in Fig. 2 *A* and 2 *B*. We find that in the region where two solutions exist, one of them is stable and one is unstable. The cross-hatched area is bounded by the ΔP versus q dependences for $L_p = R_p$ and $L_t R_t = 0$, and the one obtained if the equation for the stability criterion, Eq. 38, is set to zero, i.e., for where stable tether configurations transform into unstable ones. The stable tether configurations extend to the region (vertically hatched) of higher values of q whereas unstable ones to the region (horizontally hatched) of lower values of q. To clarify the nature of the instability of this system, the relationships between the product $L_t R_t$ and the parameter ΔP for several values of the parameter q are shown in Fig. 3. It can be seen that the region of instability is characterized by a positive slope in the relationship between $L_t R_t$ and ΔP, which corresponds to an increase in tether length upon an increase of the aspiration pressure. On the other hand, the region of stable solutions is characterized by decreasing tether length upon an increase of the aspiration pressure.

It can be seen in Fig. 3 that the experimentally assessed behavior of the system may depend on how much the ratio, $k_r/k_c = q$, differs from the critical value q_c. The latter value depends on the relative volume of the vesicle and the relative pipette radius as is illustrated in Fig. 4. For decreasing vesicle volume or increasing pipette radius, q_c increases.

During an experiment with a given vesicle the only system parameter that can be adjusted is the pressure difference. Neither the pipette nor the glass bead can be exchanged in the course of the experiment. The measurable quantities are the initial outer radius of the vesicle, R_{v0}, and pressure and L_p as functions of L_t. In Figs. 5 and 6 are given the predicted (by solving Eqs. 21, 22, 13, and 11) relationships between Δp or L_p and L_t, for different values of the system parameters and for values of the ratio $q = 2$ or 4. All calculations are performed for three values of the effective force. It can be seen that the

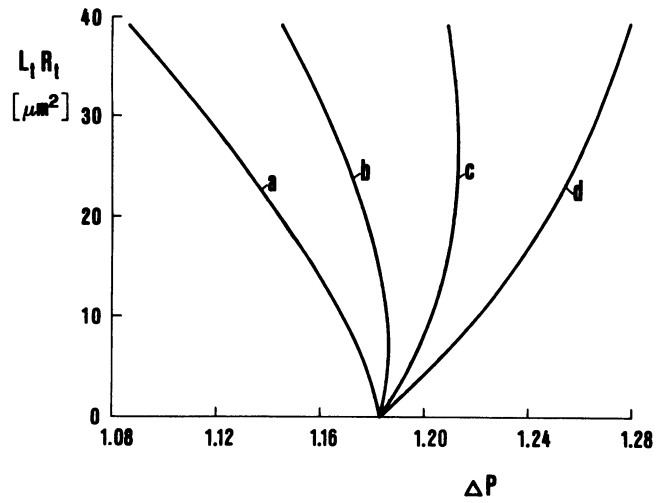

FIGURE 3 The diagram shows the product of the tether length and radius as a function of ΔP as obtained for a given q from Eqs. 24 and 25 (expressed by relative quantities). The relative volume of the vesicle is $v = 0.7$ and relative pipette radius is $R_p/R_0 = 0.4$. The four curves correspond to four different values of the ratio $q = k_r/k_c$ indicated with arrows in Fig. 2 *B*. From left to right, $q = 0.60$ (*a*), 0.45 (*b*), 0.30 (*c*), and 0.15 (*d*). The stable states correspond to the part of each curve where the product $L_t R_t$ is decreasing as a function of ΔP. Maximum $L_t R_t$ value corresponds to $L_t = R_t$ and it is obtained by eliminating R_v from Eqs. 11 and 24 (it does not depend on q).

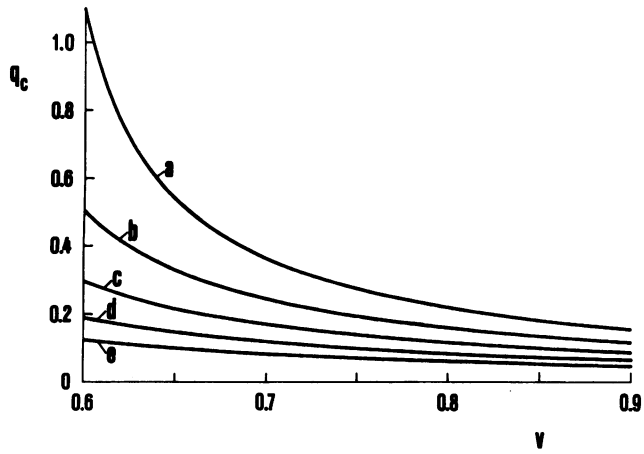

FIGURE 4 The dependence of critical ratio q_c on relative volume v for five values of relative radii of the pipette, R_p/R_0 = 0.40 (*a*), 0.37 (*b*), 0.34 (*c*), 0.31 (*d*), and 0.28 (*e*).

absolute value of the slope in the L_p/L_t diagram is larger for smaller effective forces. This reflects the fact that at smaller effective force the radius of tether is larger, and therefore more area from the pipette region is used for tether formation for the same change of L_t. Comparison of Figs. 5 *A* and 6 *A* shows that the larger is q the more curved is the dependence of L_p on L_t. Depending on the value of q and the length of the tether, this curvature may or may not be detectable experimentally. Figs. 5 *B* and 6 *B* show that the larger the effective force, the larger is the initial pressure difference. Also, the dependence of Δp on L_t is steeper at larger effective forces, and for larger values of q. At q approaching infinity, i.e., where it is not possible to expand the areas of the two layers relative to each other, the tether can not be formed.

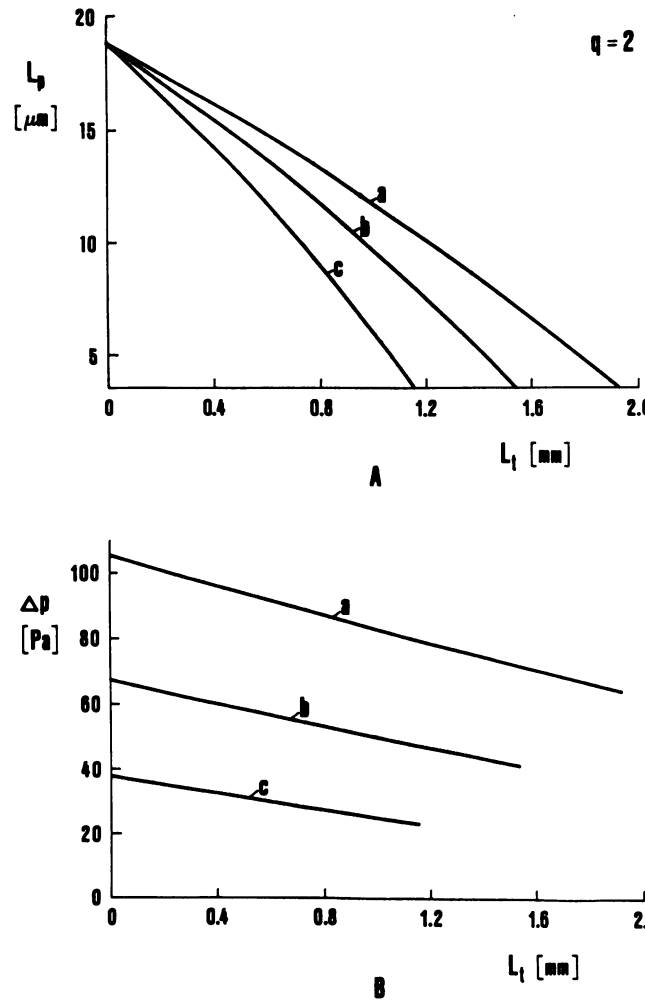

FIGURE 5 (*A*) The dependence of the length of the projection of the vesicle into the pipette (L_p) on the length of the tether (L_t) (at equilibrium) for three different values of the effective force, $f_{eff} = 5 \times 10^{-11}$N (*a*), 4×10^{-11}N (*b*), and 3×10^{-11}N (*c*). Area of the vesicle is $4\pi \times 100\ \mu m^2$ and relative volume $v = 0.75$. The radius of the pipette is taken to be 3.5 μm. The membrane material constants are: $k_c = 1 \times 10^{-19}$ J and $k_r = 2 \times 10^{-19}$ J. (*B*) The difference between the pressure surrounding the vesicle and pressure in the pipette as a function of the tether length for the same three different effective forces. The curves end where $L_p = R_p$.

DISCUSSION

Elastic behavior of phospholipid membranes is usually described by their resistance to area expansion and to bending (Evans and Needham, 1987). The present theoretical analysis focuses on the realization that in treating bilayer membranes that form closed surfaces, it is necessary to take into consideration the possibility of relative expansion (or compression) of the two constituent layers. The energy corresponding to relative area expansion can be deduced by recognizing that the two layers of the bilayer can deform elastically and independently of each other, but that they are geometrically constrained because they must remain in close contact (Svetina et al., 1985). An analogous expression for nonlocal bending was introduced by Evans (1980). It has been suggested previously (Svetina and Žekš, 1989) that the relative expansivity of the constituent layers of a bilayer could be important in determining the shapes of closed membranes. If the system is unsupported and otherwise unconstrained, a given shape can be specified by requiring that the two layers be unstressed. However, when external forces are applied, the two membrane leaflets may be unequally stressed, and the elastic

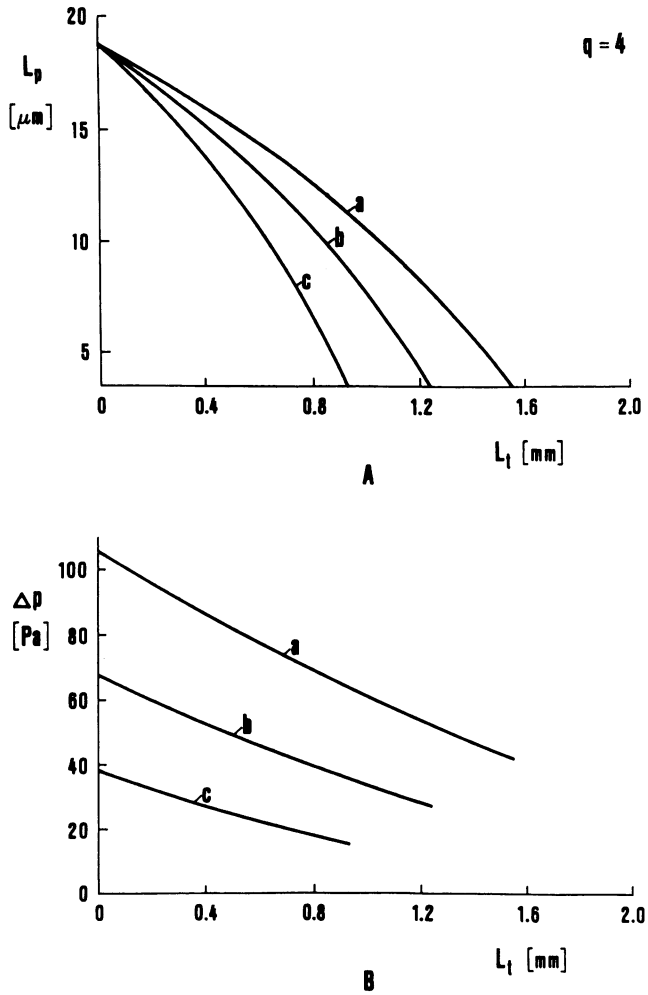

FIGURE 6 The same as Fig. 5, except $k_r = 4 \times 10^{-19}$ J.

response of a vesicle will be determined in part by the relative expansivity of the membrane. This investigation represents an analysis of one such application of external forces, namely, the formation of a membrane tether from a micropipette-aspirated phospholipid vesicle. The contribution from relative area expansion is recognized, and predictions made for the elastic response of the membrane.

The geometrical approximation of the aspirated tethered vesicle was introduced to estimate the values of the system parameters for which tethers can exist. The tether can exist if there is an equilibrium among all the forces involved. To obtain such an equilibrium, the minimum of the free energy was sought where the elastic energy of the system included membrane bending, membrane area expansivity, and the relative expansivity of the two membrane layers. This analysis was simplified in the sense that only the significant contributions to the energy were included. This enabled us to derive the necessary relationships in an analytical form. As is shown by the analysis in Appendix 1 this simplification is justified.

Besides the analysis of the equilibrium of the system, stability analysis was also performed. An important result of the stability analysis is that not all tether configurations obtained by the equilibrium analysis are stable. In particular, consideration of the bending energy alone does not yield stable tethered vesicles. This means that other elastic modes, i.e., the relative expansivity, must be included in the interpretation of the phenomenon. The nonlocal bending modulus must be finite because at its infinite value, i.e., at constant difference between the areas of the two membrane layers, the tether can not be formed.

From the described analysis of a tethered vesicle it is clear that its behavior also depends on L_t^*. The occurrence of this parameter is the consequence of the initial difference between the areas of the two membrane layers. This difference depends on how the vesicle was formed and on its history. When a vesicle is aspirated such that the portion outside the pipette is spherical, the difference between the areas of the two layers is, in general, not the same as the initial difference between these areas in the unsupported vesicle. The difference in the areas could be either larger or smaller than for the unsupported state. In one case, the external leaflet is compressed in the initial aspirated configuration, and the internal leaflet is expanded. In this case, a smaller force is needed to form the tether than in the case of $L_t^* = 0$. Thus, in this case $L_t^* > 0$. In the other case we have correspondingly $L_t^* < 0$. The value of L_t^* determines the effective forces on which the slopes in Figs. 5 and 6 depend, and uncertainties in this value can lead to scatter in the values of the parameters determined experimentally from these slopes (Waugh et al., 1992).

This analysis provides a formal basis for interpreting membrane tether formation experiments in terms of intrinsic membrane properties. Several aspects of the tether formation process not considered in detail previously have been incorporated into the analysis. Specifically, the contribution of relative area expansivity to the equilibrium conditions during tether formation has been established. In addition, the effects of constitutive differences in the areas of the opposing layers have also been included via the parameter L_t^*. Finally, predictions have been made for functional relationships among the experimentally measured parameters. Thus, this analysis is an essential step for properly interpreting tether formation experiments and for understanding the physical basis of membrane behavior in mechanical deformation.

APPENDIX 1

A more detailed model for the estimation of the bending energy of aspirated tethered vesicle

We would like to test the validity of the approximations used in this paper to evaluate the membrane bending energy of the aspirated tethered vesicle. This will be accomplished by comparing the magnitude of the neglected contributions with those that were kept in the approximation. The model treated here is more detailed geometrically in that it includes a segment of a torus as the connection between the spherical part of the vesicle and the tether (Fig. A 1). The importance of the contribution to the bending energy of this region is evaluated. The vesicle is therefore composed of the cylinder with the hemispherical cap in the pipette, the spherical section, the toroidal section, and the cylindrical tether with a hemispherical cap.

The membrane bending energy is given by Eq. 4. The total bending energy is the sum of the bending energies of the vesicle parts: the bending energy of the hemispherical cap within the pipette (W_{hp}), the bending energy of the cylinder within the pipette (W_p), the bending energy of the spherical section (W_v), the bending energy of the section of the torus (W_s), the bending energy of the cylindrical tether (W_t), and the bending energy of the hemispherical cap of the tether (W_{ht}). The membrane elastic energy is the sum of membrane bending energy and energy due to relative expansivity

$$W_{el} = \frac{k_c}{2}\int (c_1 + c_2)^2 dA_0 + \frac{k_r}{2A_0h^2}(\Delta A - \Delta A_0)^2, \quad \text{(A1)}$$

where ΔA_0 is the difference between areas of the two leaflets when the vesicle is aspirated in the pipette before the tether is made, and h is the distance between neutral planes of the layers. We assume here that the equilibrium difference between these two areas of the leaflets is equal to the initial equilibrium difference between areas in the unsupported vesicle (ΔA_0), which means that the areas of the leaflets of the aspirated vesicle are not relatively expanded (or compressed) before the tether is made (i.e., $L_t^* = 0$). The area expansivity term is neglected because its contribution to the membrane energy is small. We estimated that for the area expansivity modulus 0.2 J/m^2 (Evans and Needham, 1987) the changes in the area expansivity energy in increasing L_t from zero to 1 mm are less than five percent of the corresponding changes in the relative expansivity energy and less than one percent of the corresponding changes in the bending energy.

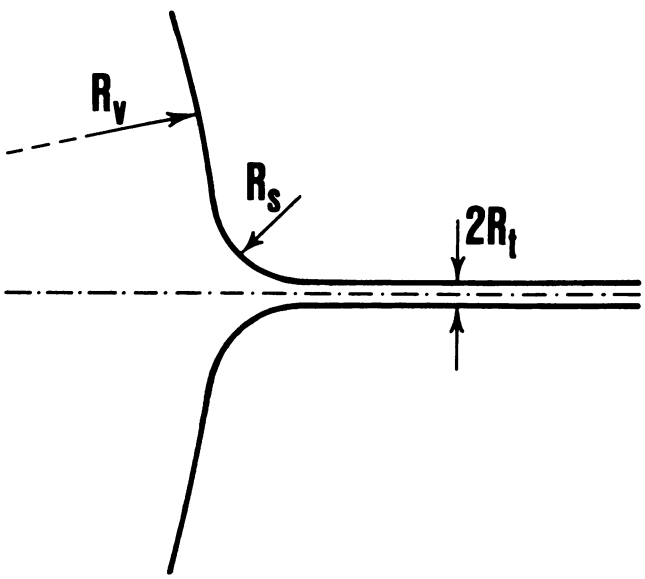

FIGURE A1 Schematic representation of the segment of the torus between the spherical part of the vesicle and tether. Notations given in the figure are: vesicle radius (R_v), torus radius (R_s), and tether radius (R_t).

The free energy of the system is

$$F = \pi k_c \left\{ 7 + \frac{L_p}{R_p} + \frac{L_t}{R_t} + \frac{2(R_t - R_s)^3}{R_s\sqrt{(R_t - R_s)^2 - R_s^2}} \cdot \operatorname{arctg}\left[\frac{(R_t - 2R_s)\left\{1 - \frac{R_t - R_s}{R_v - R_s}\right\}}{\sqrt{(R_t - R_s)^2 - R_s^2}\sqrt{1 - \left\{\frac{R_t - R_s}{R_v - R_s}\right\}^2}} \right] + \frac{4\sqrt{R_v^2 - R_p^2}}{R_p} \right\} + \frac{k_r}{2A_0h^2}(\Delta A - \Delta A_0)^2 - L_p\pi R_p^2 \Delta p - xf, \quad \text{(A2)}$$

where Δp is the difference between the pressure surrounding the vesicle and in the pipette, and

$$x = \sqrt{R_v^2 - R_p^2} + R_v\sqrt{1 - \left\{\frac{R_t - R_s}{R_v - R_s}\right\}^2} + L_t + R_t \quad \text{(A3)}$$

is the distance between pipette and the end of the tether and f is the force pulling the tether.

To obtain the shape of the vesicle we minimize the free energy with respect to the length of the projection in the pipette, the vesicle radius, the radius of the torus, and the tether length and radius. The radius of the pipette is taken to be constant. The total volume of the vesicle and the total area of the bilayer are fixed ($V = V_0, A = A_0$). The pressure in the pipette and the force pulling the tether are also fixed.

The total volume of the vesicle equals

$$V = \pi\left\{\frac{2}{3}R_t^3 - \frac{1}{3}R_p^3 + R_p^2L_p + R_t^2L_t - (R_t - R_s)R_s^2 \arccos\frac{R_t - R_s}{R_v - R_s} + \frac{1}{3}\left((2R_v^2 + R_p^2)\sqrt{R_v^2 - R_p^2} + \sqrt{1 - \left\{\frac{R_t - R_s}{R_v - R_s}\right\}^2} \cdot [2R_v^3 + 2R_s^3 + (R_t - R_s)^2(R_v - R_s)]\right)\right\}. \quad \text{(A4)}$$

Analogously, the area of the vesicle is

$$A = 2\pi \left\{ R_t^2 + R_p L_p + R_t L_t + R_v \sqrt{R_v^2 - R_p^2} + (R_v^2 - R_s^2) \sqrt{1 - \left(\frac{R_t - R_s}{R_v - R_s}\right)^2} + (R_t - R_s) R_s \arccos \frac{R_t - R_s}{R_v - R_s} \right\}. \quad \text{(A5)}$$

The difference between the areas of the two membrane leaflets is

$$\Delta A = 2\pi h \left\{ 2R_p + 2R_t + L_p + L_t + \sqrt{R_v^2 - R_p^2} + 2(R_v - R_s) \sqrt{1 - \left(\frac{R_t - R_s}{R_v - R_s}\right)^2} - R_p \arccos \frac{R_p}{R_v} - (R_t - R_s) \arccos \frac{R_t - R_s}{R_v - R_s} \right\}. \quad \text{(A6)}$$

The toroidal radius R_s is shown as a function of L_t in Fig. A2. Note that the dependence of R_s on L_t is not strong. The bending energies of each region of the vesicle for three different tether lengths are tabulated in Table A1. Because the bending energy of the tether is several orders of magnitude bigger than the contributions to the bending energy of the other parts, the approximation used in this paper is justified. The bending energy of the section of the torus is small in comparison with the bending energy of the cylindrical tether because the value of the curvature of the torus is comparable to the value of the curvature of the tether only within a very small region near the connection between these two vesicle parts. The section of the torus can be omitted in the approximation of the aspirated tethered vesicle also because R_s only slightly depends on the length of the tether (Fig. A2).

An analogous calculation reveals that the change in the bending energy at the entrance to the pipette is an order of magnitude smaller than the change in energy at the tether junction. This is because the membrane curvature at the pipette entrance changes very little during tether formation. Thus, this contribution to the energy change during tether formation can also be neglected.

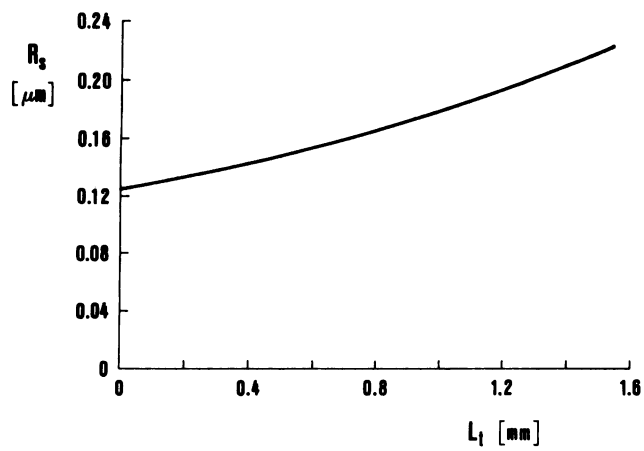

FIGURE A2 The torus radius is presented as a function of the tether length at a constant force in the tether ($f_{eff} = 4 \times 10^{-11}$N). The curve is obtained by varying the difference between the pressure surrounding the vesicle and the pressure in the pipette. The relative volume is $v = 0.75$ and the total area is $A = 4\pi \times 100\mu m^2$. The radius of the pipette is taken to be 3.5 μm. The membrane bending modulus is $k_c = 1 \times 10^{-19}$ J and the nonlocal bending modulus is $k_r = 2 \times 10^{-19}$ J.

TABLE A1 **The bending energies of the parts of the vesicle at three different values of the length of the tether in units of the bending energy of a sphere**

L_t [mm]	0	0.5	1
W_{hp}	0.5	0.5	0.5
W_p	0.5405	0.3930	0.2205
W_v	0.9545	0.9564	0.9584
W_s	0.3169	0.3426	0.3765
W_t	0	3665	6710
W_{ht}	0.5	0.5	0.5

The total area of the vesicle, the relative volume and the membrane material constants are the same as in Fig. A2.

This work was partially financed by the United States-Yugoslav Joint Fund JF-888.

Received for publication 4 April 1991 and in final form 25 October 1991.

REFERENCES

Bo, L., and R. E. Waugh. 1989. Determination of bilayer membrane bending stiffness by tether formation from giant, thin-walled vesicles. *Biophys. J.* 55:509–517.

Cooper, M. S., A. H. Cornell-Bell, A. Chernjavsky, J. W. Dani, and S. J. Smith. 1990. Tubulovesicular processes emerge from *trans*-golgi cisternae, extend along microtubules, and interlink adjacent *trans*-golgi elements into a reticulum. *Cell.* 61:135–145.

Dabora, S. L., and M. P. Sheetz. 1988. The microtubule-dependent formation of a tubulovesicular network with characteristics of the ER from cultured cell extracts. *Cell.* 54:27–35.

Evans, E. A. 1974. Bending resistance and chemically induced moments in membrane bilayers. *Biophys. J.* 14:923–931.

Evans, E. A. 1980. Minimum energy analysis of membrane deformation applied to pipet aspiration and surface adhesion of red blood cells. *Biophys. J.* 30:265–284.

Evans, E. A., and R. M. Hochmuth. 1976. Membrane viscoplastic flow. *Biophys. J.* 16:13–26.

Evans, E. A., and D. Needham. 1987. Physical properties of surfactant bilayer membranes: thermal transitions, elasticity, rigidity, cohesion, and colloidal interactions. *J. Phys. Chem.* 91:4219–4228.

Hochmuth, R. M., N. Mohandas, and P. L. Blackshear, Jr. 1973. Measurement of the elastic modulus for red cell membrane using a fluid mechanical technique. *Biophys. J.* 13:747–762.

Hochmuth, R. M., H. C. Wiles, E. A. Evans, and J. T. McCown. 1982.

Extensional flow of erythrocyte membrane from cell body to elastic tether. II. Experiment. *Biophys. J.* 39:83–89.

Song, J., and R. E. Waugh. 1990. Bilayer membrane bending stiffness by tether formation from mixed PC-PS lipid vesicles. *J. Biomech. Engr.* 112:235–240.

Svetina, S., M. Brumen, and B. Žekš. 1985. Lipid bilayer elasticity and the bilayer couple interpretation of red cell shape transformations and lysis. *Stud. Biophys.* 110:177–184.

Svetina, S., and B. Žekš. 1989. Membrane bending energy and shape determination of phospholipid vesicles and red blood cells. *Eur. Biophys. J.* 17:101–111.

Waugh, R. E. 1982a. Surface viscosity measurements from large bilayer vesicle tether formation. I. Analysis. *Biophys. J.* 38:19–27.

Waugh. R. E. 1982b. Surface viscosity measurements from large bilayer vesicle tether formation. II. Experiments. *Biophys. J.* 38:29–37.

Waugh, R. E., and R. M. Hochmuth. 1987. Mechanical equilibrium of thick, hollow, liquid membrane cylinders. *Biophys. J.* 52:391–400.

Waugh, R. E., J. Song, S. Svetina, and B. Žekš. 1992. Monolayer coupling and curvature elasticity in bilayer membranes by tether formation from lecithin vesicles. *Biophys. J.* 61:974–982.